EXPERIMENTAL INVESTIGATION OF 3D RC EXTERIOR JOINT RETROFITTED WITH FULLY-FASTENED-HAUNCH-RETROFIT-SOLUTION

Marchisella A.*[,1], Muciaccia G.[2], Sharma A.[3], Eligehausen R.[4]

Abstract

In recent years, the use of post-installed anchors to connect the haunch elements with the structural members has been investigated proficiently. It represents a promising alternative for strengthening of joints of existing reinforce concrete (RC) structures (moment resisting frames) with low invasion. The efficacy of the fully-fastened-haunch-retrofit (FFHR) solution has been proven by past works for two-dimensional RC beam-to-column joints, subjected to cyclic loading, without transverse beam and slab. In these cases, the presence of the haunch, providing a suitable design of the anchoring system, modifies the strength hierarchy shifting the mode of failure from joint's shear breakout to the formation of the plastic hinge in the beam. However, due to the presence of the slab and transverse beam, as the authors discussed elsewhere, an increase both (i) in the joint resistance and (ii) in the beam flexural resistance must be expected, but particular care must be taken to the non-symmetric behavior. In this regard, results obtained for two RC beam-to-column sub-assemblies with transverse beam and slab retrofitted using FFHR are presented. The structural behavior under cyclic load is compared with the as-built identical specimen. The

*Corresponding author
[1]PhD Candidate, Department of Civil and Enviromental Engineering, Politecnico di Milano, Italy, angelo.marchisella@polimi.it
[2]PhD, Ass. Prof., Department of Civil and Environmental Engineering - Politecnico di Milano, giovanni.muciaccia@polimi.it
[3]PhD, Jun. Prof., Institut für Werkstoffe im Bauwesen - Universität Stuttgart, akanshu.sharma@iwb.uni-stuttgart.de
[4]PhD, Prof., Institut für Werkstoffe im Bauwesen - Universität Stuttgart, eligehausen@gmx.de

AAM Engineering Structures" - https://doi.org/10.1016/j.engstruct.2021.112206

applicability of the FFHR to existing RC structures, is confirmed but, at high level of ductility demand, both anchorage break-down and reduced displacement capacity are observed.

Key words: , Beam-to-Column-Joint, Slab, Haunch-Retrofit-Solution, Steel-to-Concrete Connections

2010 MSC: 00-01, 99-00

---

1. Introduction

1.1. Background

Retrofit of existing RC frames, deficient in lateral-load carrying capacity have been a challenge since new regulations accounting to seismic rules details have completely changed the way of design and finally lead the pending question on what to do with existing structures built over the past 60 years [1, 2]. Under lateral loads, the most deficient structural part for a RC frames is represented by the beam-to-column joint. Several attempts of retrofit, by different authors, have been made in the last fifteen years using haunch retrofit solution, which consists in introducing steel angles at the joint to reduce the shear load transferred in the joint core. The relevant studies are listed in Table 1. The search strategy sought only studies published in English. The main search terms were haunch, retrofit, reinforced concrete, beam-to-column joint. Mainly, the test configuration is a two-dimensional sub-assembly beam-to-column joint exterior configuration, tested under displacement control in quasi-static condition. In[3] a two-dimensional frame structure with one bay and two-stories, 2/3 scaled, is tested using shaking table. Same test method is used in [4] and [5] however here 1/3 scaled frame is considered with the addition of slabs and transverse beams. Post-installed anchors are used to fasten the metallic haunch to the RC structure in most of the cases. Instead, collars (encasement of both beam and column, connected with a diagonal prop) are used in the oldest works. While the latter technique has the advantage of avoiding weakening at the haunch location [6], the issue of invasiveness and practical implementation is higher if

compared with fully-fastened-haunch-retrofit (FFHR). As for the results: (i) in all the cases the relocation of the plastic hinge to the main beam and the avoidance of joint shear failure is achieved at least in one experiment; (ii) the enhancement of load carrying capacity is expected to be, in average, approximately the 50% of the control specimen (if it is declared as "seismic deficient" or equivalently "designed for gravity loads only") with the ±8% of variability; (iii) the previous estimate cannot be applied for shaking table tests where damage assessment is performed rather than ductility analysis; (iv) in case of anchorage failure increase in the load-carrying capacity is obtained anyway.

1.2. Research Significance

The presented work addresses a set of four Beam-To-Column Joint sub-assembly with slab and transverse beam, tested against cyclic loads. Two specimens are tested in the as-built conditions. Two specimens are retrofitted with Fully-Fastened-Haunch-Retrofit-Solution (FFHR) using different fastening technologies. Results for the as-built specimen have been published elsewhere[7], and here partially re-discussed. In the context of the works related to the topic of FFHR, this investigation, aim to introduce the novelty of the influence of the slab and transverse beam in the seismic performance of the retrofitted sub-assembly. The plan of the paper is as follow: (i) in section titled "Experimental details", specimen preparation and test method are presented; (ii) in section titled "Experimental Results" all the results for the of the work are summarized.

2. Experimental Details

2.1. Experimental Program

Four different specimens have been constructed, representing a sub-detailed three-dimensional beam-to-column joint in a reinforced concrete building, including the presence of a transversal beam and of a solid slab. The sub-assembly is retrofitted with steel haunches fastened to the joint via post-installed anchors. The test matrix is reported in Table 2. The specimen labeled S01 was

used mainly to tune the test apparatus and S02 should be considered as the "reference" for the as-built condition, [7]. The following detail, regarding the specimens' preparation, are valid for all the specimens indiscriminately.

2.2. Specimen Details

2.2.1. Beam-To-Column sub-assembly

The geometry of the sub-assembly and the reinforcement layout are illustrated in Figure 1. The specimen has (i) 300 mm wide by 450 mm deep main beam and (ii) square column with 350x350 mm cross-section. The slab is 150 mm thickness and the transverse beam has 350x450 mm cross-section. The slab reinforcement (two layers ϕ12 with 150 mm spacing) extended to the back of the transverse beam with straight anchorage. The deformed longitudinal bars in the beam were anchored inside the joint after bending them by 90°. Net concrete cover of 3 cm is adopted.

2.2.2. Steel Haunches

The haunch elements used for retrofitting of the specimen consisted of three steel plates that are welded together (see Figure 1). The steel grade was S275, the plates' thickness is 16 mm and the diameter of the hole is 20 mm. Each side of the haunch has three rows of fasteners at a distance of 150 mm and 100 mm along the long and the short side, respectively. The holes were slotted to overcome the interference of the rebars during the drilling operation. The length of the slots are 60 mm and 50 mm, being the last associated to the outermost fasteners. Same element was adopted in [3]. Within the context of the presented experimental campaign, the haunch design is based on the following assumptions: (a) the diagonal element (in tension) remains elastic under the application of the maximum force that anchors group can transmit; (b) in compression buckling is avoided by modelling it as fixed ends with compact rectangular cross-section; (c) considering the same load condition as for the diagonal, yielding of the base plate is avoided. Further details considering the

dependant behavior of the anchor group with respect the plate's thickness[8] are given in the following.

2.2.3. Anchorage System

The plot of the retrofit procedure is given in Figure 2. Specimen S01, S03 and S04 were tested adopting FFHR, assuming different anchorage systems. Specifically, in S01 a retrofit trial was made using bonded anchors having 130 mm as embedment depth, the bonding agent is an epoxy resin characterized by a mean value of the bond strength $\tau_{cr,m}$=5.0 MPa in cracked concrete, considering wide crack opening (w =0.8 mm) for the seismic condition [9][10]. In S03, a bonded concrete screw is used. The only relevant application of an anchor of the same type is recognized in [11]. The anchor is made with a M16 stainless steel rod of 290 mm length including the screwed part, the smooth shank and the hexagonal head. The anchor has been modified in order to accommodate the test condition (haunch thickness and installation of the washer load cells), whit respect its original configuration (Figure 2.e). In particular, the hexagonal head was cut and the shank was threaded with metrical pitch, i.e. 2 mm. The final configuration of the anchor is composed by concrete screw developed for 90-95 mm; (ii) 60 mm of smooth bar; (iii) at least 100 mm of threaded end. In S04, bonded anchors are used (threaded rods and epoxy mortar) with the following specifications for the embedment depths: (i) 350 mm in the column using M20 rods; (ii) passing holes in the beam/slab using M12 rods. Same bonding agent is used as in S01. The anchor group can be classified as rectangular with regular spaced anchors of the same type according to [8]. As a result, the design rules specified in [12] apply. Particularly, in case of group of anchors under tension, the prescription are primarily based on overlapping area factor according to Concrete Capacity Design method (CCD) [13]. However, in the light of the investigation on the the influece of base plate stiffness presented in [8], results show that all the anchors get activated, in a single row of 4, when the spacing-to-thickness ratio(s/t) is equal to 2.25. In this case, the load-carrying-capacity is comparable the one estimated according to CCD method. In the presented

investigation, the anchor group is characterized by a two-dimensional grid being 9.36 and 6.25 the s/t ratios, in the two directions. Being dealing with plates, the curvature involved in two different bending planes, two-dimensional anchor array must be considered stiffer than one-dimensional one. For this reason, and also accounting for the stiffening effect provided by the attached diagonal, the assumed thickness is considered sufficient to consider all the anchors participating equally in the group behavior.The anchor assessment is presented in the following section.

2.2.4. Materials

Concrete was medium workability (Class S2), maximum aggregate size 25 mm. The specimens were cast from two different batches. Standard cube (150x150x150mm) control specimens were taken from each batch and tested at 28 days after casting. The results are reported in Table 2. For the reader's convenience results for all the specimens included within the experimental campaign are reported. Rebars were of grade B500. Results of material characterization given by the manufacturer are reported in Table 3. Steel haunches have steel grade S275. The actual resistance was not determined being the nominal yield strength sufficient to satisfy overstrength requirement with respect the connected members and the fasteners group.

2.2.5. Test Setup

The test layout is sketched in Figure 3, such configuration and load condition aim to represent the simplified static behavior of the beam-to-column joint subassembly in a resisting frame system under lateral forces. Specifically, (i) the point of inflection of columns are assumed at the storey mid-height and (ii) beam point of inflection are considered at the mid-span[14]. The specimen is placed with the column aligned with the horizontal plane and the main beam in a vertical stand position.The load is applied at the beam-end using a horizontal screw actuator with a maximum capacity of 750 kN. The hinge restraints at the ends of the columns were enforced using reaction beams which were tied down to

a rigid base with a set of high strength rods. To prevent the uplift of the member ends during loading, the rods are pre-tightened. In the horizontal direction, the applied load is contrasted by steel angles bolted to the base beam. The connection between the actuator and the beam-end allowed their free relative rotation, while the out of plane displacement of the actuator was restrained. Cylindrical hinges were provided at the column ends, by placing rollers between the column face and the reaction frame, at the points below the restraining beams. Moreover, a set of PVC cylinders were placed between the contrast angles and the column faces to prevent extended contact and ensure the more efficient transfer of the horizontal reaction forces. In S01, no gap is provided between the base beam and the column. No axial force is applied to the column, being its effect outside the scope of the investigation and, furthermore, biasing the result in case of joint shear failure [15][16][17]. The specimen was dressed by LVDTs, washer load cells and strain gauges. The latter were installed on the rebars in a total number of 24. Specifically: (i) in the slab, 12 strain gauges were mounted on the top and bottom layers of longitudinal reinforcement, adjacent to the transverse beam; (ii) in the column, 6 strain gauges were placed on the reinforcing bars of the north lateral face, below and above the joint region; (iii) in the beam all the rebars were monitored. Additionally, strain gauges were also installed on the haunch diagonal plate.

2.2.6. Displacement protocol

The test is performed in displacement control. The wire transducer connected to the load collar is assumed as controlling signal, i.e. the stroke of the screwed actuator is inverted whenever the target displacement is reached. The velocity of the screwed actuator is set to 0.2 mm/s till the tar-get displacement reached the value of 35 mm, then the velocity is increased to 0.4 mm/s. A stepwise incremental displacement history was applied to the specimen as shown in Figure 4, similar to what it is proposed in [18]. The steps are labeled with the code "D0x", where the "x" index assumes values from 1 to 8. Each step comprises two consecutive cycles.

3. Experimental Results

In this section the experimental results are described referring to the Figure 5 showing the load-displacement (drift) curves and the backbone curves obtained enveloping the end points of each first cycle. Additionally, in Table= 4, the backbone characterization is performed defining (i) the peak state; (ii) the conventional ultimate state [at the 20% load drop after peak];(iii) the finale state (last point reached during the test); (iv) the ductility evaluation considering an equivalent elastic-perfect-plastic system, with the same energy absorption as the backbone [19]. Crack pattern for the top side (East) of the slab and of the bottom (West) are showed in Figure 6 and Figure 7, respectively. An overview of the failure modes, characterizing the different specimens is given in Figure 8.

3.1. As built specimens: S01 and S02

As can be inferred from Figure 5 and also in Table 4, S01 and S02 are characterized by (i) the same flexural crack pattern for the beam/slab and torsional behavior of the transverse beam; (ii) almost equal level of load at the first joint shear crack, (iii) different evolution approaching both the peak and the ultimate load.

First, flexural cracks approximately spaced by 100 or 120 mm forms at the top (East) side of the slab-beam and at bottom (West) when the load direction is positive and negative, respectively. Shear cracks are also present in the beam in the vicinity of the load application points. The column shows mixed flexural and shear cracks. Inclined cracks associated with the torsional behavior characterize the transverse beam. After reaching the first joint shear crack and for subsequent levels of drift flexural and torsional cracks widen almost without any further crack occurrence [Figure 7].

Second, despite the failure surface cannot be completely characterized, due to the presence of the transverse beam, a detachment between the column and the main beam is recognized for a drift level almost equal to 1%. Such evidence, both in case of positive and negative direction is defined as first joint shear crack.

It is worth mentioning that, aside from the bending behavior which is partially responsible for the crack growth, it may be confirmed that an X-shaped failure surface creates passing through the joint region as shown, in case of S02, in Figure 8.c/d. After its formation, the crack continuously widen for subsequent drift levels. The final damage pattern of the joint, discerned after lifting the specimens, is characterized by the spalling of concrete surrounding the bents of the beam's longitudinal rebars.

Third, the absence of gap between the base beam and the column contributes to an enhancement in load-carrying-capacity, after reaching high level of drift (greater than 1%). Under such circumstance, the vertical reaction provided by the base beam would be significant to the point that the joint confinement is promoted. As a result, the peak load in S01 is higher with respect S02 and no load drop is observed in case of negative and positive load direction, respectively. Nevertheless, the different boundary condition in S01 leads to an increase in column's shear as confirmed by a pronounced inclined crack which start propagating from the joint face as demonstrated in Figure 8.In the comparisons pertinent with the section "Discussion", S01 will be discarded since (i) no further level of ductility demand after 4% of have been tested and (ii) because the different boundary conditions, at those drift levels, may affect the structural behavior.

Finally, for S02, converting the backbone curve into an equivalent elasto-plastic behavior, ductility values of $\mu = 3.45$ and 2.51 are obtained in case of positive and negative direction, respectively. Even though, its definition might be questioned, because high pinching phenomena characterizes the hysteretic behavior.

3.2. Retrofitted specimens

3.2.1. S01

An attempt of retrofit, using FFHR, has been carried out for the specimen S01 after the as-built test. The damaged concrete is chiseled and substituted with high-strength repairing mortar. The haunch is then fasten to the concrete

using bonded anchors whit 130 mm embedment depth. A reduced test protocol is performed targeted to ±1%, ±2% and finally ±6%. The test is performed with gap between base beam and the column. The retrofit intervention is able to restore the load carrying-capacity up to a drift level equal to 2%. Subsequently, the anchorages failure and the mortar breaking is observed and the specimen starts behave as the as-built approaching its post-peak branch. Nonetheless, a residual capacity of 100 kN is recognized both in positive and negative load direction.

3.2.2. S03

As showed in Figure 6 and Figure 7, the crack pattern is characterized by the absence of torsional cracks for the transverse beam and the occurrence of flexural cracks (1 additional crack whit respect the as-built condition) in the slab/beam, for drift level less than 2%, i.e. D04. Cracks, also concentrate in the vicinity of all the anchors, in the case of negative direction of the load.

The peak load in positive direction, corresponds to the anchorage failure at the East side, in the column [Figure 8.f]. The latter, is characterized by anchorages break-out. Specifically, two rows of anchorages formed a combined concrete-cone and pullout failure. The depth of the concrete cone is 70 mm, with a corresponding anchor's displacement approximately equal to 20 mm. At the West side, anchorages in the beams failed subsequently being (i) the load in positive direction and (ii) the drift level the same, i.e. 2%. The failure at the West side is also confirmed by the reading of the load cells, which are showed in Figure 9. Looking for the most stressed anchor [label 5NWB], it reaches almost the load value of 40 kN, then it drops during step D05. The same conclusion, can be sustained analyzing the strain gauge measuring the local state of deformation for the haunch diagonal plate.

The post-peak is characterized by the development of torsional cracks in the transverse beam, and with all the probability the promotion of the joint shear failure notwithstanding higher load level with respect S02 due to the resistance offered by the compressed haunch.

Due to the abrupt load drop after anchorage failure, it's rather difficult to define (with energy equivalence) the equivalent elasto-plastic behavior, consequently the ductility is given only for the negative direction of the load, i.e. $\mu = 2.51$.

3.2.3. S04

S04 shows the same behavior of S03 up to the drift level of 2%, notwithstanding a reduced stiffness, in positive direction, due to a not-voluntarily cycle at a drift level of 1% conducted before performing the test.

The anchorage failure is successfully avoided and the specimen overcomes the lateral load-carrying capacity obtained in S03, obtaining 285 kN and 206 kN in positive and negative direction, respectively. Anchors in the beam (passing holes) are active both in positive and in negative direction, varying the load distribution among the anchor group passing from drift levels lower than 2% until the ultimate state [Figure 9, plots 1NWB and 5NWB]. Anchors in the columns show one-directional reaction and a non-constant load distribution among the group for drift level higher than 2%. The central anchor [labeled 2NWC] is the most loaded reaching almost 100 kN, for drift levels higher than 4%. Strain gauges reading [Figure 9, plots HW1-HW2], reveal that exists a quasi-uniform distribution of tensile strains within the diagonal width, up to the drift level of -4%. After such threshold, HW2 reduces whereas HW1 remains almost constant.

At the level of the sub-assembly, the post-peak behavior is characterized by severe damage attributable to reduced rotational capacity of the plastic hinge. In particular, for the positive direction, crushing compressed concrete contemporary to the buckling of rebars are observed leading to a final ductility value equal to $\mu = 2.60$. Conversely, in case of negative load the ductility is 3.34. Rigorously, being the final load level not below the 80% of the peak, the ductility here indicated is a lower estimate. Nevertheless, it is recognized that the application of a tensile strain to the previously buckled rebars might lead, also in this case, to a reduction of the rotational capacity.

4. Discussion

4.1. Hysteretic behavior

Analysis of cyclic behavior is performed considering as relevant parameters: (i) the energy dissipated during cycles; (ii) the secant stiffness degradation of subsequent cycles with respect the first cycle of step D01; (iii) the impairment of strength between two consecutive cycles at the same drift level. Results are shown in Figure 10. In S02, an un-stable behavior is evident, namely the difference of the dissipated energy, at same drift, is higher than 20%. Such evidence is partially confirmed by the evolution of the impairment of strength. Reduced energy absorption can be also related to the bond-slip behavior characterizing the beam longitudinal bars. In fact, considering the anchorage length-to-diameter ratio (l_{bd}/d_{bl}) a value 12.6 is obtained which leads to a condition prone to bond failure, having considered the value of 10 as lower limit [20]. In case of the retrofitted specimens, the behavior is stable up to a drift level equal to 3%. Only in case of S04, the stability is maintained for higher level of the drift demand. Although specimens are characterized by different failure mechanisms, they show a comparable stiffness reductions and impairment of strength. This is inherent in the definition of the secant stiffness which is mainly affected by the cracking state. The overall response is not significantly affected by the bond-slip mechanism due the reduction of the tensile force acting in the proximity of the anchorage length as a consequence of the moment reduction and of the relocation of the plastic hinge. Additionally, it is proven that the value of the stiffness reduction is lower than 0.5 for drift value in between 2% and 4%, for which collapse states should be assessed in design.

4.2. Local state of deformation

The strain profile for the slab/beam is given in Figure 11 for all the specimens. The plot scale, on the vertical axis, is set to -5000 to +5000 $\mu\epsilon$ being almost 2500 $\mu\epsilon$ the yielding value. Strain gauges reading are reported until they reach out-of-scale.

Considering the positive direction of the load, only one rebar in the slab has comparable level of strains with respect to the beam. The latter leads to the conclusion that the effective width of the slab can be reasonably assimilated to the the width of the beam increased by the depth of the slab on each side slightly contradicting the provision in [21] which considers for the same case two times the slab depth as additional width. The difference might be significant in case of the evaluation of the moment curvature relationship for the cross-section. It is worth mentioning that, both top and bottom layer of reinforcement in the slab show the same behavior.

Under negative direction, the beam rebars (bottom layer) yield after 3% and 2% value of the imposed drift for as-built and retrofitted specimens, respectively. This can be expected due to the increased stiffness of the sub-assembly.

4.3. Anchors Assessment

Bonded anchors were used to fasten the haunch to the sub-assembly whit different embedment depth in S03 and S04 (S01-retrofit will be not considered in this discussion). In case of S03 combined pullout and concrete cone (PO+CC) has been observed both in the column and in the beam/slab. In case of S04, despite the evidence of inclined cracks related to the formation of cone mechanism, anchor failure has been prevented. In both of the case, in fact concrete cone should be considered not decisive since the stirrups, even tough not specifically designed for the purpose, could be considered as activated [22]. In Table 5 results of the estimate of PO+CC load-carrying capacity and concrete cone supported by stirrups legs are presented. Reference to the mean values of the material parameters is made. Evaluation of the force acting as tensile force on the group of six anchors is retrieved from finite element model using frame elements for the beams, the columns, the haunch and shell elements for the slab. Static analysis, are carried out using linear-elastic material. Resistances are evaluated according to [12]. In PO+CC a value of $\tau = 0.5\tau_{cr}$ is used being τ_{cr} the minimum bond strength necessary to switch to pure concrete cone mechanism. The resulting bond strength values can be considered reliable in case of

cracked concrete if compared with relevant literature [23][24]. For the purpose of the following discussion, drift level of 3% and negative direction of the load are considered. Similar result can be obtained for the positive direction.

What does emerge from this assessment is that in S03 the acting force is higher than the estimated resistance confirming that the solution is prone to failure. However, the discrepancy between acting forces (at peak) and resistance PO+CC can be attribute to one, or all, the following reasons: (i) the linear-elastic structural analysis might not be able to reproduce the correct internal forces at high ductility demand leading to an over-estimate; (ii) the fasteners belonging to the group might behave differently due to different crack condition, i.e. the outermost with respect the joint suffer high cracks ;(iii) an higher value of bond strength could be assumed, although a more severe reduction factor for the overlapping areas and group effect is expected in this case.

Maintaining the same hypothesis on structural analysis and resistance evaluation, in S04 the load-carrying capacity in case of PO+CC is higher than the acting force.

Finally, in both cases considering the activation of 3 stirrups (6 legs in total of diameter equal to 10 mm), concrete cone is not decisive being the yielding strength higher than PO+CC and the acting force.

4.4. Design Recommendations

To promote beam hinging, in the design of the haunch retrofit, the flexural capacity evaluation must include the slab participation, because it increases the beam resistant moment and, in turn, (i) the shear forces in the elements,(ii) the joint shear demand and the (iii) anchorage pullout force. In case the flexural strength ratio between resistant moments of the column and the beam (with slab) at the end section of the haunch is less than 1.3 [21], the lateral strength and stiffness of the column might be ignored in the design of the lateral load resisting system as it is allowed in [25], proving that the presence does not introduce less conservative results (that is, torsional effect). If the abovementioned requirement was not satisfied, haunch retrofit should be combined with other

retrofit techniques (FRP, jacketing) aiming at increasing the flexural capacity of the column[26]. The same applies in case the column or beam or both becomes shear critical. Nevertheless, including the slab in the capacity assessment might be beneficial for the success of the retrofit because it increases the joint shear resistance (in case of transverse beam is present [27]) and it excludes the edge proximity at least for one side of the anchorage to the concrete.

5. Conclusions

The presented paper details the experimental results for the FFHR of a beam-to-column joint with slab and transverse beam in which bonded concrete screw (embedment depth equal to 150 mm, both in the column and in the slab/beam) and bonded anchors using threaded rods (embedment depth equal to 300 mm in the column and passing holes in the beam/slab) were used to fasten the haunch to the RC sub-assembly. Specimens have been tested up to 5% of drift level. Results have been compared with as-built specimen which failed in joint shear at 2.9% of drift level. The following conclusions and design recommendations can be drawn:

1. Both an increase of the load-carrying capacity of the sub-assembly and changes in the cyclic behavior and in mode of failure are observed.

2. The joint shear failure is prevented as long as the anchorage capacity is not exceeded. The latter suggest, in force based design, the application of an overstrength factor which must be calibrated specifically for the adopted anchorage type.

3. Anchorage failure has been obtained in the case bonded concrete screws fastening at 2.1% of drift level . The failure was characterized by the combined pull-out and shallow cone development. Comparison with analytical prediction confirmed the condition prone to failure.

4. In case of bonded anchors (threaded rods), the response is characterized by beam hinging development. In the very last part of the test,after 4.0%

of drift level, bending failure of the cross-section was reached, characterized by break-out of the compressed part accompanied with buckling of compressed rebars. A reduced ductility associated to lack of rotational capacity in both the direction of the loading has been observed. The latter condition should be considered peculiar in case of 3D joints in which the slab contributes to the resisting moment.

5. The effect of slab participation has a great impact in the design of the retrofit, because it affects all the other actions within a frame. The enhanced beam flexural strength results in an increased joint shear demand and anchorage capacity. However, beneficial effects such as the improved resistance of the joint should be taken into consideration.

6. Acknowledgments

The support in carrying out the experiments of the Testing Lab. for Materials, Buildings and Civil Structures of the Politecnico di Milano is gratefully acknowledged. The authors wish to extend their gratitude to company Adolf Würth GmbH & Co. KG for partially financing the experimental program.

7. Conflict of interest

The authors declare no conflict of interest.

8. References

References

[1] Priestley N. Displacement-based seismic assessment of reinforced concrete buildings. Journal of Earthquake Engineering 1997;1(1):157–92. doi:10.1080/13632469708962365.

[2] El-Attar AG, White RN, Gergely P. Behavior of gravity load designed reinforced concrete buildings subjected to earthquakes. ACI Structural Journal 1997;94(2):133–45.

[3] Sharma A. Seismic Behavior and Retrofitting of RC Frame Structures with Emphasis on Beam-Column Joints – Experiments and Numerical Modeling. Phd thesis; University of Stuttgart; 2013.

[4] Ahmad N, Akbar J, Rizwan M, Alam B, Khan AN, Lateef A. Haunch retrofitting technique for seismic upgrading deficient RC frames. Bulletin of Earthquake Engineering 2019;17(7):3895–932. URL: https://doi.org/10.1007/s10518-019-00638-9. doi:10.1007/s10518-019-00638-9.

[5] Akbar J, Ahmad N, Rizwan M, Javed S, Alam B. Response Modification Factor of RC Frames Strengthened with RC Haunches. Shock and Vibration 2020;2020. doi:10.1155/2020/3835015.

[6] Akbar J, Ahmad N, Alam B. Response Modification Factor of Haunch Retrofitted Reinforced Concrete Frames. Journal of Performance of Constructed Facilities 2020;34(6):04020115. doi:10.1061/(asce)cf.1943-5509.0001525.

[7] Marchisella A, Muciaccia G, Sharma A, Eligehausen R. Experimental Investigation on Beam-To -Column Joint with Slab and Transverse Beam under Cyclic Loading. In: 5th Workshop "The New Boundaries of Structural Concrete – NBSC 2019" (Milan, Italy). Milano: San Marino: ImReady; 2019, p. 283–92.

[8] Bokor B, Sharma A, Hofmann J. Experimental investigations on concrete cone failure of rectangular and non-rectangular anchor groups. Engineering Structures 2019;doi:10.1016/j.engstruct.2019.03.019.

[9] Eligehausen R, Mallèe R, Silva JF. Anchors In Concrete Structures. Ernst And Sohn; 2006.

[10] Hoehler MS, Eligehausen R. Behavior and testing of anchors in simulated seismic cracks. ACI Structural Journal 2008;105(3):348–57.

[11] Lechner J, Feix J. Development of an efficient shear strengthening method for dynamically loaded structures. In: 11th fib International PhD Sym-

posium in Civil Engineering. Tokyo: Federation International Du Beton; 2016,.

[12] EN1992-4 . Eurocode 2 Design of Concrete Structures - Part 4 Design of Fastenings for Use in Concrete. 2018.

[13] Fuchs W, Eligehausen R, Breen J. Concrete Capacity Design (CCD) Approach for Fastening to Concrete. ACI Structural Journal 1995;109(January):1–4.

[14] Fardis MN. Seismic Design, Assessment and Retrofitting of Concrete Buildings. London: Springer; 2009. ISBN 9781402098413.

[15] Park S, Mosalam KM. Parameters for shear strength prediction of exterior beam-column joints without transverse reinforcement. Engineering Structures 2012;36:198–209. URL: http://dx.doi.org/10.1016/j.engstruct.2011.11.017. doi:10.1016/j.engstruct.2011.11.017.

[16] Vollum R, Newman JB. Strut and tie models for analysis/design of external beam-column joints. Magazine of Concrete Research 1999;51(6):415–25. doi:10.1680/macr.1999.51.6.415.

[17] Bakir PG, Boduroğlu HM. A new design equation for predicting the joint shear strength of monotonically loaded exterior beam-column joints. Engineering Structures 2002;24(8):1105–17. doi:10.1016/S0141-0296(02)00038-X.

[18] ACI . ACI 374.2R-13 Guide for testing Reinforced Concrete Structural Elements under Slowly Applied Simulated Seismic Loads. Tech. Rep. 2; American Concrete Institution; 2015.

[19] Park R. Evaluation of Ductility of Strucuters and Structural Assemblages from Laboratory Testing. Bulletin of the New Zealand National Society for Earthquake Engineering 1989;22(3):155–66. URL: https://bulletin.nzsee.org.nz/index.php/bnzsee/article/view/774. doi:https://doi.org/10.5459/bnzsee.22.3.155-166.

[20] Kaku T, Asakusa H. Bond and anchorage of bars in reinforced concrete beam-column joints. ACI Special Publication 1991;123:401–24.

[21] EC8 . Eurocode 8: Design of Structures for earthquake resistance. 2004.

[22] Sharma A, Eligehausen R, Asmus J. Analytical Model for Anchorages with Supplementary Reinforcement Under Tension or Shear Forces. In: Where technology and engineering meet; vol. 1. Maastricht: Springer. ISBN 9783319594712; 2017,doi:10.1007/978-3-319-59471-2.

[23] Eligehausen R, Balogh T. Behaviour of Fasteners Loaded in Tension in Cracked Concrete. ACI Structural Journal 1995;92(3):365–79.

[24] Eligenhausen R, Cook RA, Appl J. Behavior and design of adhesive bonded anchors. ACI Structural Journal 2007;104(5):645–6.

[25] ACI . ACI 318-19 Building Code Requirements for Structural Concrete and Commentary. 2019. ISBN 9781641950565. doi:10.14359/51716937.

[26] Raza S, Khan MK, Menegon SJ, Tsang HH, Wilson JL. Strengthening and repair of reinforced concrete columns by jacketing: State-of-the-art review. Sustainability (Switzerland) 2019;11(11). doi:10.3390/su11113208.

[27] Pantazopoulou S, French C. Slab Participation in Practical Design of R.C. Frames. ACI Structural Journal 2001;(June):479–89.

[28] Pampanin S. Development and validation of a metallic haunch seismic retrofit solution for existing under-designed RC frame buildings. Earthquake Engineering and Structural Dynamics 2006;44(September):657–75. doi:10.1002/eqe. arXiv:arXiv:1403.5481v1.

[29] Chen Th. Retrofit strategy of non-seismically designed frame systems based on a metallic haunch system. Msc thesis; University of Canterbury; 2006.

[30] Sharbatdar M, Kheyroddin A, Emami E. Cyclic performance of retrofitted reinforced concrete beam-column joints using steel prop. Construction

and Building Materials 2012;36:287–94. URL: http://dx.doi.org/10.1016/j.conbuildmat.2012.04.115. doi:10.1016/j.conbuildmat.2012.04.115.

[31] Genesio G. Seismic Assessment of RC Exterior Beam- Column Joints and Retrofit with Haunches Using Post-Installed Anchors. Ph.D. thesis; University of Stuttgart; 2012.

[32] Sharma A, Reddy GR, Eligehausen R, Genesio G, Pampanin S. Seismic Response of Reinforced Concrete Frames with Haunch Retrofit Solution. ACI Structural Journal 2014;.

[33] Dang Ct, Dinh Nh. Experimental Study on Structural Performance of RC Exterior Beam-Column Joints Retrofitted by Steel Jacketing and Haunch. Advances in Civil Engineering 2017;2017(i).

[34] Kanchanadevi A, Ramanjaneyulu K. Non-Invasive Hybrid Retrofit for Seismic Damage Mitigation of Gravity Load Designed Exterior Beam–Column Sub-Assemblage. Journal of Earthquake Engineering 2019;0(00):1–26. URL: https://doi.org/10.1080/13632469.2019.1592790. doi:10.1080/13632469.2019.1592790.

[35] Marchisella A. Beam-To-Column Joint with Slab and transverse beam Retrofitted with Fully-Fastened Haunch Retrofit Solution (Technical Report - Unpublished). Tech. Rep.; Politecnico di Milano; 2019.

[36] Moncarz PD, Krawinkler H. Theory and Application of Experimental Model Analysis in Earthquake Engineering (Technical Report). Tech. Rep. 50; Department of Civil and Environmental Engineering Stanford University; University of Standford; 1981.

[37] Bonacci J, Wight JK. Displacement-based assessment of reinforced concrete frames in earthquakes. ACI Special Publication 1996;162(6):117–38.

9. TABLES

Table 1: Relevant studies on RC Beam-to-Column Joint retrofitted using haunch

First Author	**Structure**	**n.test**[a]	**Scale fact.**[b] (-)	**Fast. Techn.**[c]	**Type of test**[d]	**Failure**[e] (-)	**Drift Lev.**[f] (%)	**Reference**
Pampanin	Ext Joint	3 (1)	0.67	Collar	QS	BH	4%	[28]
Chen	Corner Joint	1 (1)	0.67	Collar	QS	BH	3%	[29]
Sharbatdar	Ext Joint	2 (2)	0.50	Collar	QS	BH	5%	[30]
Genesio	Ext Joint	2 (1)	0.67	PI	QS	BH	3%	[31]
Genesio and Sharma	Ext Joint	5 (1)	1.00	PI	QS	BH+JS+AN	3%	[32]
Sharma	2D portal 1bay/2Story	1 (1)	0.67	PI	ST	-	-	[3]
Dang and Troung	Ext Joint	1 (1)	0.50	PI	QS	BH+JS	3%	[33]
Kanchanadevi	Ext Joint	2 (1)	1.00	PI/Collar	QS	BH+JS	4%	[34]
Ahmad	2D portal 1bay/2Story	-	0.33	PI	ST	-	-	[4]
Akbar	2D portal 1bay/2Story	2(1)	0.33	AC	ST	AN	3%	[5]
Marchisella	Ext. Joint with slab	2 (2)	1.00	PI	QS	BH+JS+AN	5%	[35]

[a] Number of test on the retrofitted specimen, in round brackets the number of control specimens (without retrofit).

[b] Scaling factor used for the geometry and other quantity usually defined according to [36].

[c] [collar] is a system of steel plates encasing the structural member (beam or column); [PI] Post-Installed fasteners; [AC] after casted haunch with post-installed rebars.

[d] [QS] quasi-static test and [ST] shaking table test.

[e] Failure mode obtained in the retrofitted specimen, i.e [BH] Beam Hinging and [JS] Joint shear failure and [AN] Anchorage failure.

[f] Highest ultimate drift level (according to [37]) obtained in testing the retrofitted specimens.

Table 2: Test Matrix for BTJ

Code and Condition		**Anchors**	f_{ccm} [(a)]	**Notes/References**
S01	As Built and FFHR	-	27.9	(b)
S02	As Built	-	27.0	See [7]
S03	FFHR	Concrete Screws	39.1	
S04	FFHR	Bonded Anchors	37.7	-

[a] Concrete cubic strength at the test day.

[b] Specimen was mainly used to test the efficiency of the test setup.

Table 3: Reinforcement bars yielding stress characterization

Yield stress (f_{ym}) in MPa					
ϕ**10**	ϕ**12**	ϕ**16**	ϕ**20**	ϕ**22**	ϕ**25**
530	490	520	520	530	530

Table 4: Test Results

Test	Loading Direction	Peak		0.80 Peak		Final		Ductility[a]				Failure mode[b]
		F_{max} (kN)	Δ_{max} (%)	$F_{0,80}$ (kN)	$\Delta_{0,80}$ (%)	F_{fin} (kN)	Δ_{fin} (%)	F_y (kN)	Δ_y (%)	μ_y (-)	Energy (kN·m)	
S01[c]	(+)	142,3	2,9	131,2	4,1	131,2	4,1	-	-	-	-	JS
	(-)	131,7	2,9	120,3	4,1	97,2	4,1	-	-	-	-	JS
S02	(+)	148,3	3,3	111,3	3,3	68,0	6,1	111,0	1,6	3,45	12,4	JS
	(-)	112,5	2,1	96,1	3,3	56,1	6,1	93,0	2,1	2,51	9,3	JS
S03	(+)	229,5	2,1	176,4	4,1	163,2	5,1	-	-	-	-	ANCH +JS
	(-)	192,5	2,1	155,4	4,1	124,6	5,1	155,0	2,0	2,51	15,6	ANCH
S04	(+)	285,0	4,1	238,3	5,1	191,7	6,1	250,0	2,3	2,60	28,5	BH
	(-)	206,2	4,1	-	-	188,4	7,6	205,0	2,0	3,34	27,4	BH

[a] Evaluated using area equivalence, according to [19].

[b] [JS] Joint shear failure; [ANCH] Anchorage failure; [BH] Beam hinging.

[c] Results are referred to the as-built condition.

Table 5: Anchor Assessment

	Test			Notes
	S03	S04		
Acting force				
Drift lev.	3.0%		-	
N	182	182	kN	
Resistance				
Combined Pullout and Concrete Cone				
d	16	20	mm	Diameter
h_{ef}	150	300	mm	Embedment depth
Ψ_g	1.35	1.43	-	Group factor
Ψ_s	0.93	0.88	-	Proximity of an edge factor
Ψ_e	1.00	1.00	-	Eccentricity factor
$A_{p,N}/A^0_{p,N}$	2.51	1.67	-	Overlapping area factor
τ_{cr}	9.8	10.8	MPa	Bond strength at concrete cone
τ	4.9	5.4	MPa	Assumed bond strength
s_{cr}	259	355	mm	Shallow cone projection
N^0_r	37	111	kN	Bond strength - Single fastener
N^g_r	116	212	kN	Bond strength - Group
Concrete cone - Reinforcement				
N_{re}	250	250	kN	Considering 6 stirrups legs activated

10. FIGURES

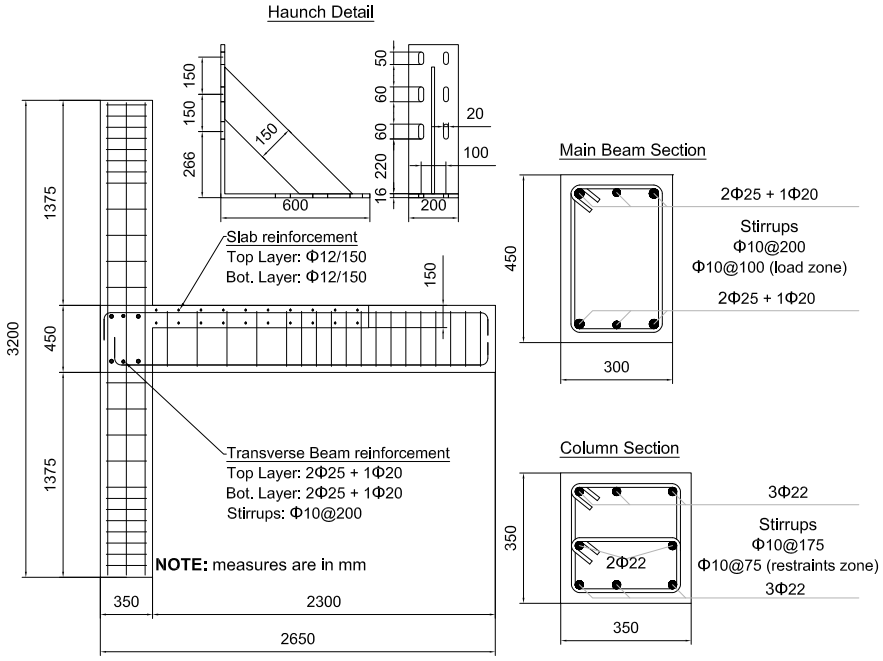

Figure 1: Specimens geometry and reinforcement layout

HAUNCH INSTALLATION

(a) Holes drilling using diamond drill core or hammer or both.

(b) Haunch fastening after mortar levelling.

FASTENING

(c) Slot filled with mortar.

(d) Pre-torque clamping.

(e) Concrete Screw used in S03.

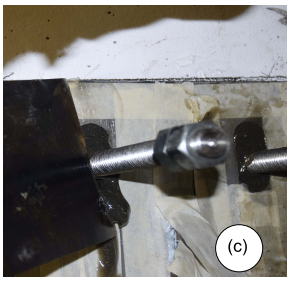

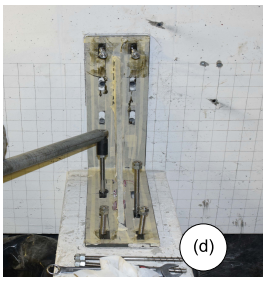

ANCHORS DETAILS

Test	Fastener	h_{ef} - Column	h_{ef} - Beam/Slab
S01	Bonded	130 mm	130 mm
S02	-	-	-
S03	Screw (e)	150 mm	150 mm
S04	Bonded	300 mm	Passing Through

NOTE. (h_{ef}) Embedment Depth

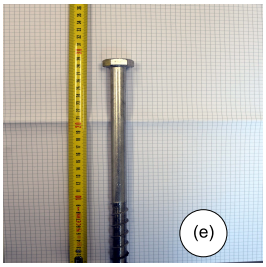

Figure 2: Haunch installation and fastening details

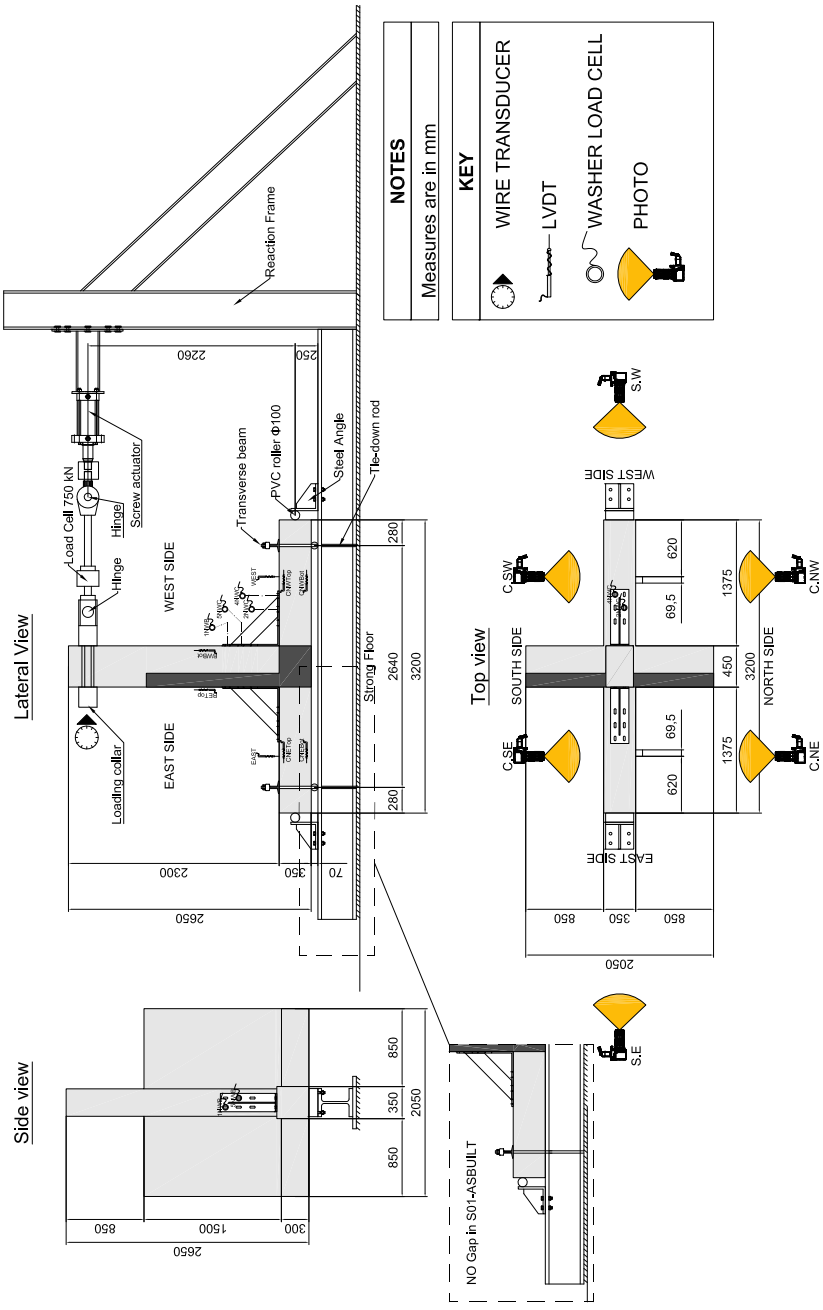

Figure 3: Details of the test setup

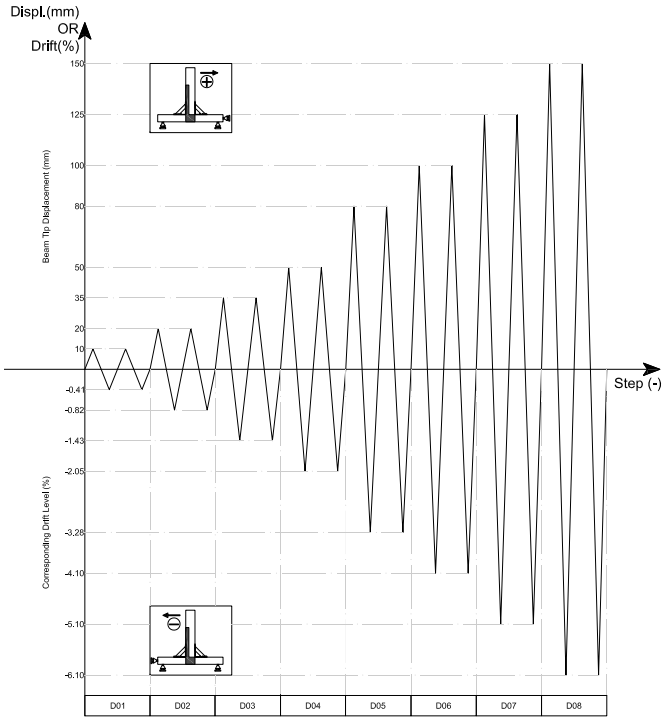

Figure 4: Test Protocol

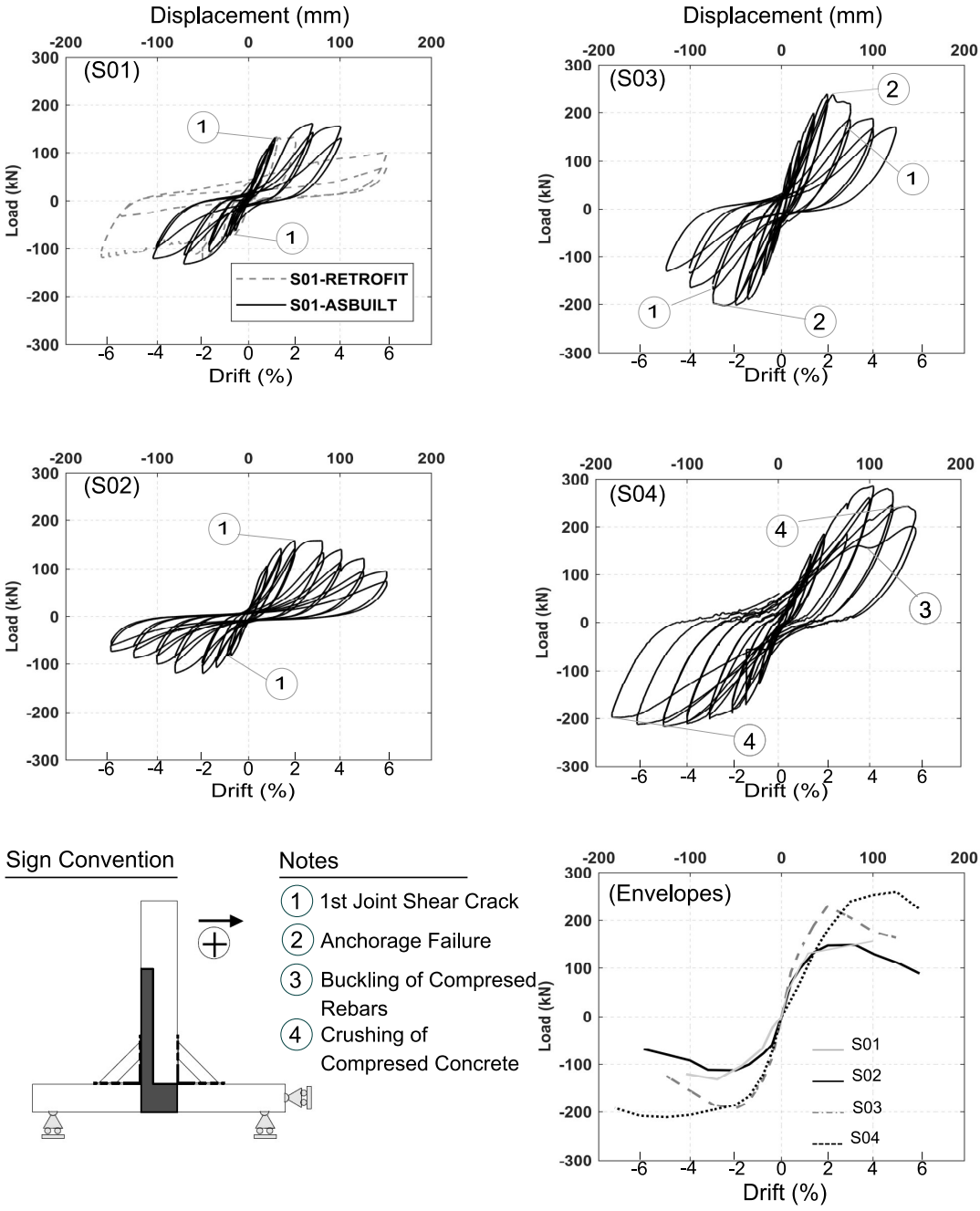

Figure 5: Load versus displacement (drift) response and backbone curves

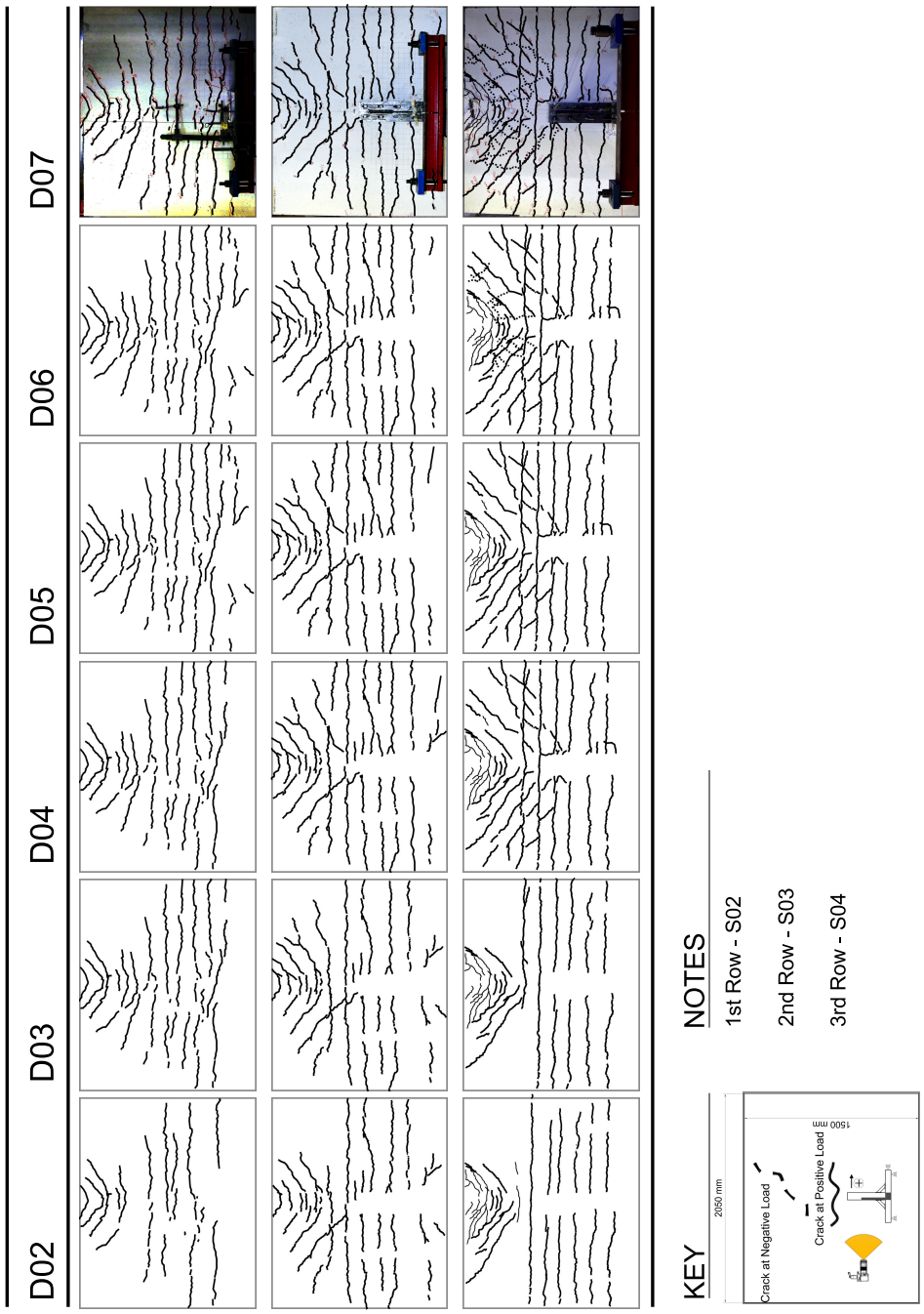

Figure 6: Crack pattern at the Top side (East) of the slab

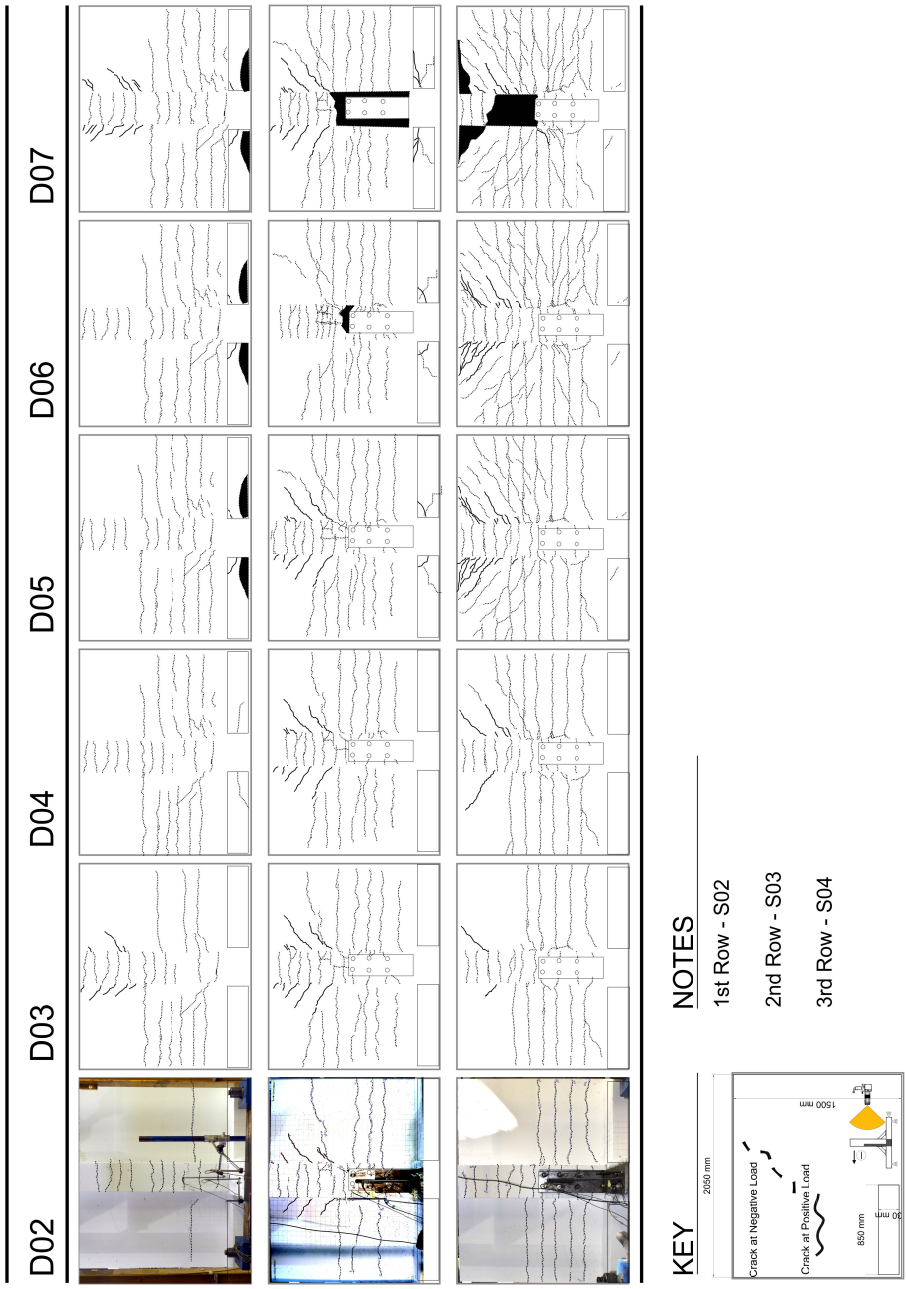

Figure 7: Crack pattern at the bottom side (West) of the slab

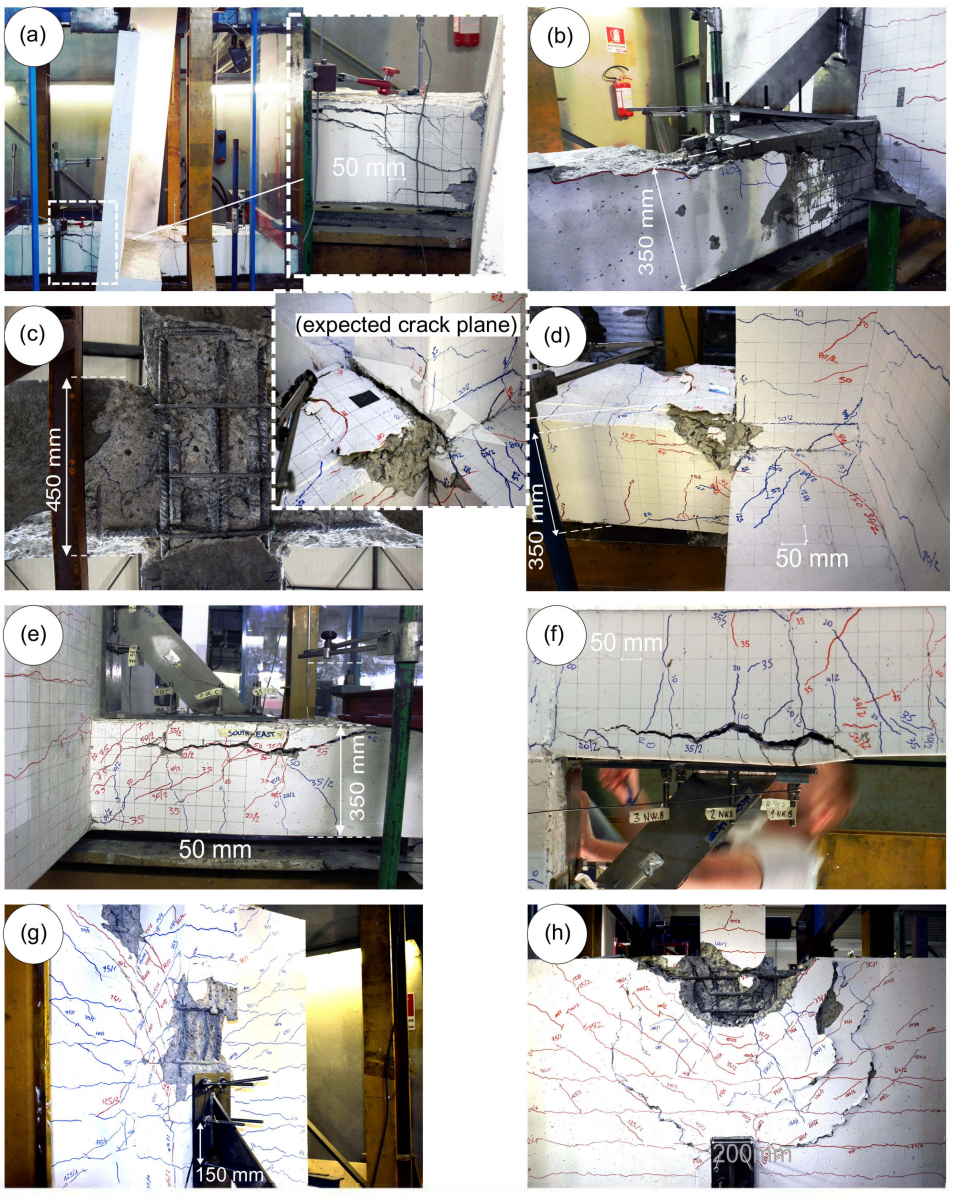

Figure 8: Mode of failure: (a) S01-As-Built, severe shear crack in the column due to the gap absence;(b) S01-Retrofit, mortar and anchorage failure; (c) S02, joint external face [transverse beam in the horizontal direction]; (d) S02, joint internal face; (e) S03, anchorage failure at the column (East); (f) S03, anchorage failure at the beam (West); (g) S04, beam hinging (West); (h) S04, beam/slab hinging (East)

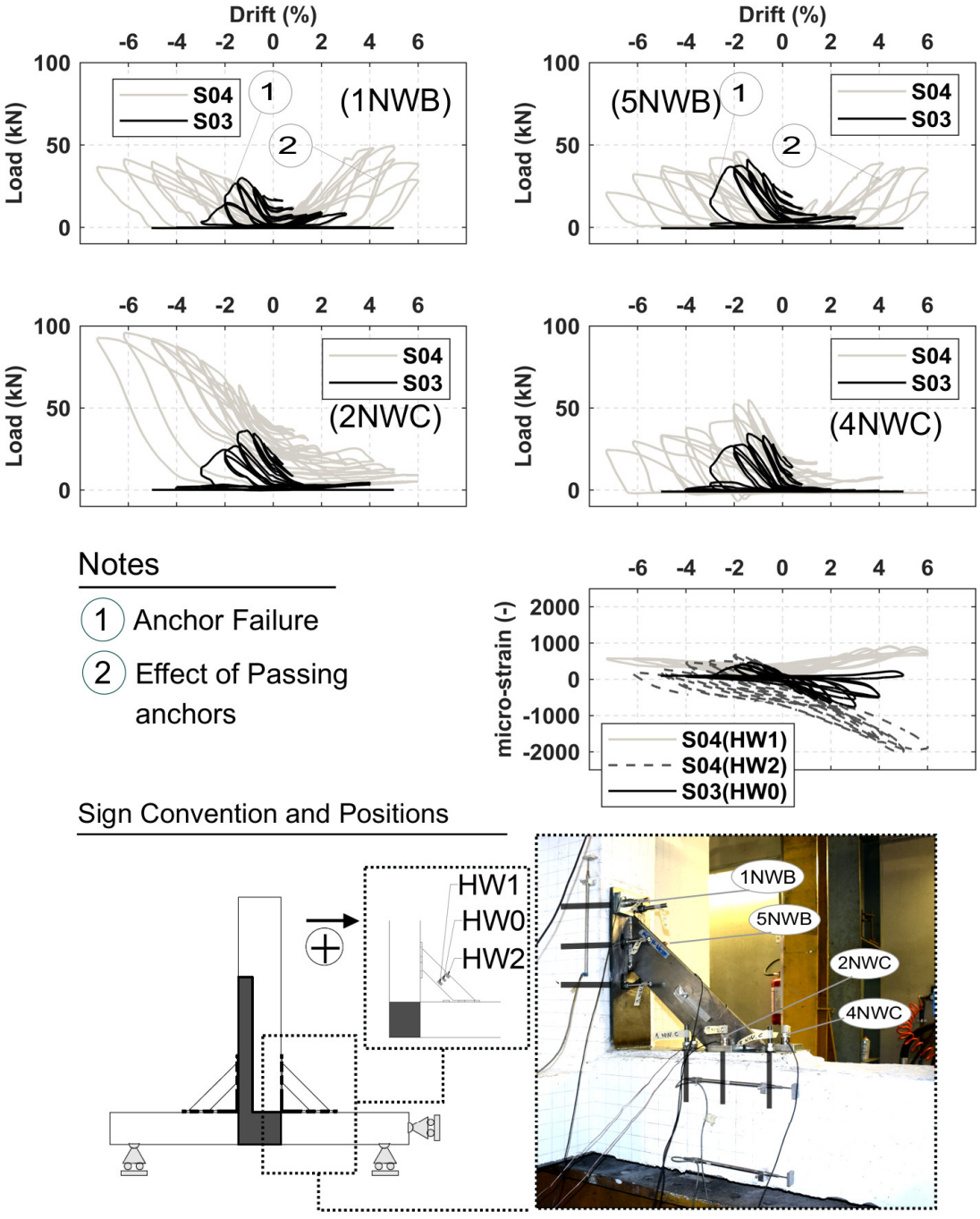

Figure 9: Anchors forces and haunch strain

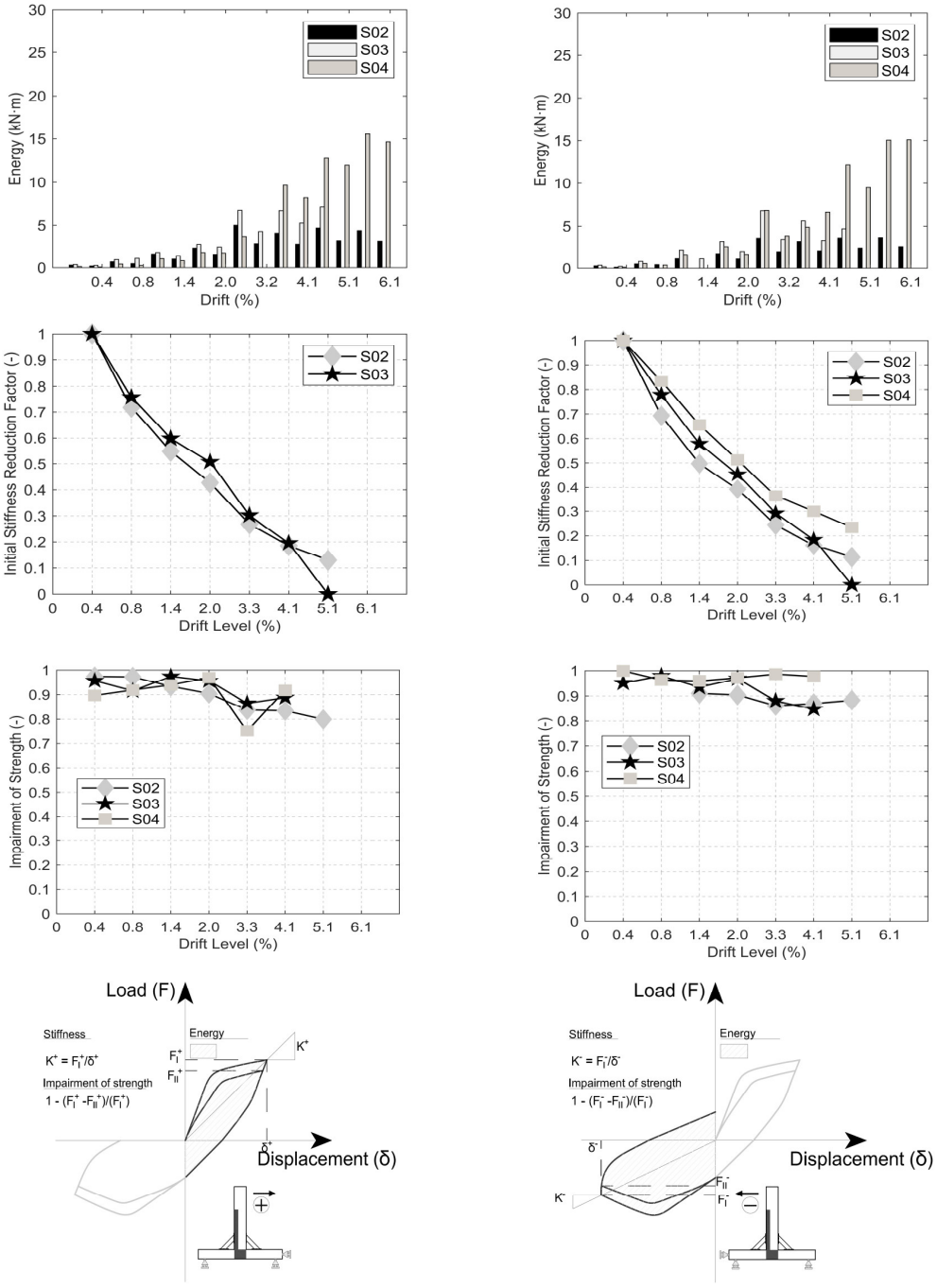

Figure 10: Hysteretic behavior: Energy, Stiffness reduction, Impairment of strength

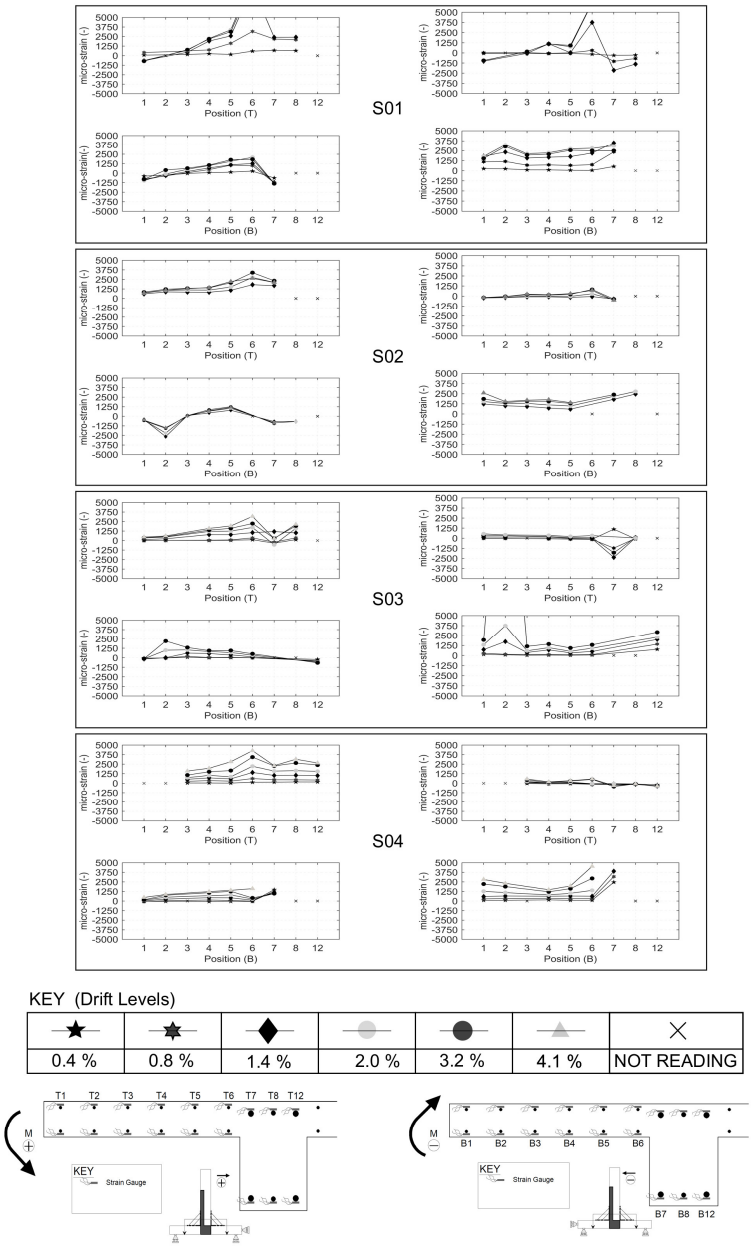

Figure 11: Strains